

**George R. Washko, Mark T. Dransfield, Raúl San José Estépar, Alejandro Diaz, Shin Matsuoka, Tsuneo Yamashiro, Hiroto Hatabu, Edwin K. Silverman, William C. Bailey and John J. Reilly**

*J Appl Physiol* 107:185-191, 2009. First published Apr 30, 2009; doi:10.1152/jappphysiol.00216.2009

**You might find this additional information useful...**

---

This article cites 22 articles, 12 of which you can access free at:

<http://jap.physiology.org/cgi/content/full/107/1/185#BIBL>

Updated information and services including high-resolution figures, can be found at:

<http://jap.physiology.org/cgi/content/full/107/1/185>

Additional material and information about *Journal of Applied Physiology* can be found at:

<http://www.the-aps.org/publications/jappl>

---

This information is current as of August 3, 2009 .

## Airway wall attenuation: a biomarker of airway disease in subjects with COPD

George R. Washko,<sup>1,6</sup> Mark T. Dransfield,<sup>2</sup> Raúl San José Estépar,<sup>3</sup> Alejandro Diaz,<sup>1,4</sup> Shin Matsuoka,<sup>5,6</sup> Tsuneo Yamashiro,<sup>5,6</sup> Hiroto Hatabu,<sup>5,6</sup> Edwin K. Silverman,<sup>1,4</sup> William C. Bailey,<sup>2</sup> and John J. Reilly<sup>1,6</sup>

<sup>1</sup>Pulmonary and Critical Care Division, Brigham and Women's Hospital, Harvard Medical School, Boston, Massachusetts; <sup>2</sup>University of Alabama at Birmingham, Birmingham, Alabama; <sup>3</sup>Surgical Planning Laboratory, Laboratory of Mathematics in Imaging, Department of Radiology, Brigham and Women's Hospital, Boston, Massachusetts; <sup>4</sup>Department of Respiratory Diseases, Pontificia Universidad Católica de Chile, Santiago, Chile; <sup>5</sup>Channing Laboratory, Boston, Massachusetts; and <sup>6</sup>Center for Pulmonary Functional Imaging, Brigham and Women's Hospital, Boston, Massachusetts

Submitted 26 February 2009; accepted in final form 25 April 2009

**Washko GR, Dransfield MT, Estépar RS, Diaz A, Matsuoka S, Yamashiro T, Hatabu H, Silverman EK, Bailey WC, Reilly JJ.**

Airway wall attenuation: a biomarker of airway disease in subjects with COPD. *J Appl Physiol* 107: 185–191, 2009. First published April 30, 2009; doi:10.1152/jappphysiol.00216.2009.—The computed tomographic (CT) densities of imaged structures are a function of the CT scanning protocol, the structure size, and the structure density. For objects that are of a dimension similar to the scanner point spread function, CT will underestimate true structure density. Prior investigation suggests that this process, termed contrast reduction, could be used to estimate the strength of thin structures, such as cortical bone. In this investigation, we endeavored to exploit this process to provide a CT-based measure of airway disease that can assess changes in airway wall thickening and density that may be associated with the mural remodeling process in subjects with chronic obstructive pulmonary disease (COPD). An initial computer-based study using a range of simulated airway wall sizes and densities suggested that CT measures of airway wall attenuation could detect changes in both wall thickness and structure density. A second phantom-based study was performed using a series of polycarbonate tubes of known density. The results of this again demonstrated the process of contrast reduction and further validated the computer-based simulation. Finally, measures of airway wall attenuation, wall thickness, and wall area (WA) divided by total cross-sectional area, WA percent (WA%), were performed in a cohort of 224 subjects with COPD and correlated with spirometric measures of lung function. The results of this analysis demonstrated that wall attenuation is comparable to WA% in predicting lung function on univariate correlation and remain as a statistically significant correlate to the percent forced expiratory volume in 1 s predicted when adjusted for measures of both emphysema and WA%. These latter findings suggest that the quantitative assessment of airway wall attenuation may offer complementary information to WA% in characterizing airway disease in subjects with COPD.

computed tomography; contrast reduction

COMPUTED TOMOGRAPHY (CT) IS being employed by multiple research groups to objectively examine airway disease in subjects with chronic obstructive pulmonary disease (COPD). Assessments of this process are based on proximal airway wall morphology and their correlation to the distal burden of small airway disease (15). These objective measures can be dependent on technically complicated algorithms that employ airway wall intensity profiles to define the lumen-wall and wall-

parenchymal boundaries of the airway wall (18, 20). Little work has been done, however, to directly examine the X-ray attenuation values within those intensity profiles.

CT imaging is based on structure density, and it is well recognized that, for objects whose dimensions are the same order of magnitude as the point spread function (PSF), their CT attenuation values will be an underestimate of actual tissue density. Termed contrast reduction, this process has been documented in both experimental and clinical applications (22, 26). In such cases, the peak CT attenuation found within the structure is a function of object size, density, and the CT scanning algorithm used to reconstruct the image. Therefore, in the context of a fixed scanning algorithm, interobject variations in peak CT attenuation values may be a direct reflection of a change in structure size and/or density. Based on this, investigators have proposed using the CT attenuation of thin objects, such as the cortical shell of vertebral bone, as an index of structural strength (5). By measuring the average of the peak CT numbers measured along the long axis of the shell, the mean of the peak CT attenuation values, one could have an objective metric of cortical shell size/strength in an object well below scanner resolution.

We postulated that the same principle of contrast reduction could be applied to the quantification of airway disease in subjects with COPD. The remodeling observed in the proximal airways of subjects with COPD (23) would result in a similar increase in the airway wall X-ray attenuation as a result of increased airway wall dimension and, potentially, density. Subjects with more advanced airway disease and thicker airway walls would, therefore, have higher measures of peak wall attenuation (PWAt). To test this hypothesis and to examine the ability of this metric to characterize the nature of a subject's expiratory airflow obstruction, we analyzed data from a subset of subjects enrolled in the National Lung Screening Trial (NLST), who underwent CT scanning and measurement of lung function at the University of Alabama at Birmingham. Some of the results of this study have been published previously in abstract form (25).

### MATERIALS AND METHODS

The study and paper were reviewed and approved according to the procedures outlined in the *NLST/LSS Publications, Presentations, and Associated Studies Working Group's Review Procedures and Authorship Guidelines*. This study also received approval from the Institutional Review Boards at both the University of Alabama at Birmingham and Brigham and Women's Hospital.

Address for reprint requests and other correspondence: G. R. Washko, Pulmonary and Critical Care Division, Dept. of Medicine, Brigham and Women's Hospital, 75 Francis St., Boston, MA 02115 (e-mail: Gwashko@Partners.org).

### Computer-based Simulation Study

The CT imaging process can be modeled by a linear system that is fully characterized by a PSF. As detailed by Dougherty and Newman (5), the PSF can be decomposed as the convolution of three different components.

$$\text{PSF-tot} = \text{PSF-1} * \text{PSF-2} * \text{PSF-3} \quad (1)$$

PSF-1 describes the geometric characteristics of the CT scanner, such as the finite width of the X-ray beam, X-ray scattering, and the linear response of the X-ray detector. PSF-2 is associated with sampling into the reconstruction grid and the finite pixel size, and PSF-3 encompasses the effect of the reconstruction kernel. Although the PSF is neither isotropic nor position independent (21), for the sake of simplicity, it can be considered to be circularly symmetric with a two-dimensional Gaussian function employed as a reasonable model of the pseudo-Gaussian PSF experimentally measured in commercial systems (5, 18, 24). Thus the resulting PSF can, therefore, be approximated by the following equation.

$$\text{PSF}(x) = \frac{1}{\sigma\sqrt{2\pi}} e^{-\frac{x^2}{2\sigma^2}} \quad (2)$$

This model, given by Eq. 2, does not include well-described nonlinear effects, like streaking artifacts and beam hardening, which were neglected for the purposes of this simulation.

An idealized airway profile can be simulated as a staircase function with three layers, each with unique intensity levels (Fig. 1). The inner layer or simulated lumen is assigned a nominal intensity of  $-1,000$  Hounsfield units (HUs) and a radius of 2 mm. The middle layer corresponding to the airway wall is varied in width and attenuation to simulate biological conditions. The outer layer represents simulated lung parenchyma with an intensity of  $-700$  HUs. For each idealized airway staircase profile, a simulated CT intensity profile can be generated by convolving the PSF (where the sigma or standard deviation = 1 mm) with the input or "true" profile. Examples are shown in Fig. 1. Using this model, the interrelation between wall attenuation, specifically, the PWAt (the peak attenuation in each of the intensity profiles), and wall thickness (WT) can be examined.

### Phantom Study

A phantom study using a range of simulated airway sizes was performed to validate the airway wall segmentation methods utilized in this investigation and to examine the influence of airway size on measures of airway wall attenuation (Fig. 2). The simulated lung phantom was created for the COPDGene Study and consists of polycarbonate tubes embedded in foam (polycarbonate density: 1.18

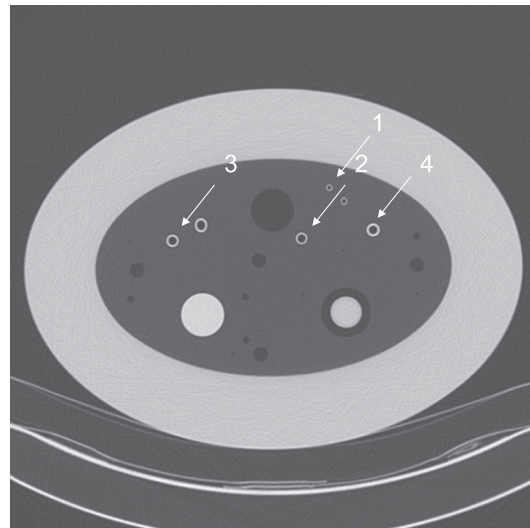


Fig. 2. Axial image of the COPDGene phantom. Four tubes representing simulated airways of a range of sizes were analyzed.

gm/ml; foam density: 0.16 gm/ml; details kindly provided by the manufacturer, The Phantom Laboratory, www.phantomlab.com). The phantom underwent CT imaging using a GE 64 slice scanner. Images were acquired using 120 kVp and a tube current of 100 mA with a gantry rotation time of 0.5 s. The scanning field of view was set at 360 mm. Images were reconstructed using a standard reconstruction algorithm with a slice thickness of 0.625 mm and interval of 0.625 mm.

Detailed information regarding image analysis is provided following the description of the clinical CT imaging protocol.

### Subject Population

Data from this study cohort have been published previously, and a full description of the NLST is available at <http://www.cancer.gov/nlst>. Briefly, the NLST is a randomized trial comparing annual chest X-rays to CT scans for the early detection of lung cancer among current and former smokers. Subjects were eligible to participate in this screening trial, if they were between the ages of 55 and 74 yr and had a minimum of 30 pack·yr of cigarette smoking. Subjects were excluded if they had a prior history of lung resection, lung cancer, or an acute respiratory infection requiring treatment with antibiotics in the previous 12 wk. Approximately 50,000 subjects were enrolled. All subjects enrolled at the University of Alabama were evaluated for

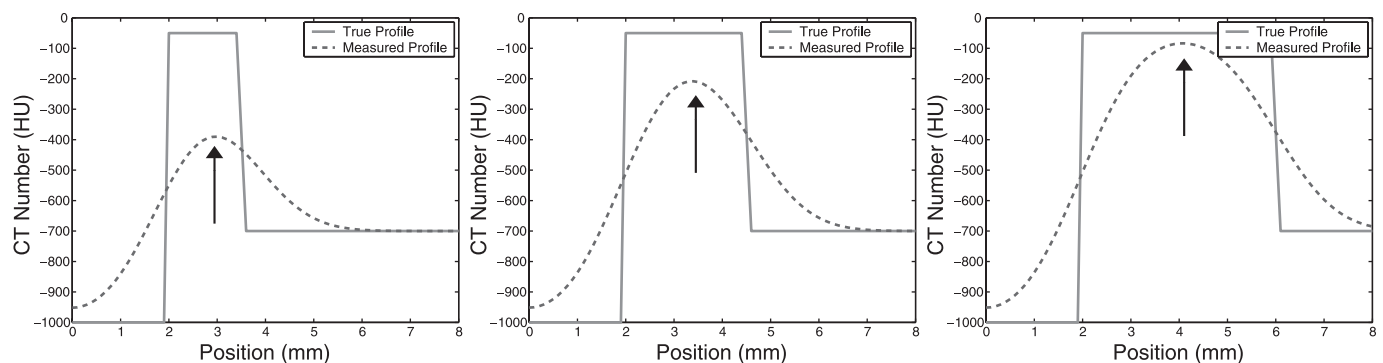


Fig. 1. Three examples of idealized airways modeled as a staircase function (true profile). In each of the three cases, the lumen was 2 mm with an attenuation of  $-1,000$  Hounsfield units (HUs), and the parenchyma was  $-700$  HUs. Left to right: the "real" airway wall is 1.5, 2.5, and 4 mm in thickness with an attenuation of  $-50$  HUs. Superimposed on these idealized models are simulated computed tomography (CT) intensity profiles (measured profile). Note that, in all cases, the measured CT peak wall attenuation (PWAt), as denoted by an arrow, does not reflect the "true" attenuation of  $-50$  HUs provided in the staircase model, but that, as the real wall thickens, the PWAt approaches the expected value of  $-50$  HUs. The arrow denotes the mean PWAt of the single-intensity profile.

participation in the current investigation, and only the 224 subjects imaged on a single CT scanner with a common reconstruction algorithm were included in this final analysis.

### Study Procedures

CT imaging of the lungs, as well as spirometry and epidemiological information, were collected under separate investigational protocols. After undergoing CT imaging per the NLST protocol, subjects providing additional informed consent performed prebronchodilator spirometry, according to American Thoracic Society standards (2, 12), and were classified using modified Global Initiative for Chronic Obstructive Lung Disease (GOLD) criteria for disease severity (17). Cigarette smoking history and current smoking status were also recorded.

**NLST CT protocol.** For all subjects, helical imaging was performed at full inflation using a GE QXi four-slice scanner. Images were acquired using 120 kV and 60 mA, with a pitch of 1.5 and a gantry rotation time of 0.8 s. The scanning field of view ranged from 270 to 460 mm, based on body habitus. Images were reconstructed using the Standard GE algorithm with a 2.5-mm slice width at 2-mm intervals.

**Computer-based simulation analysis.** A total of 861 profiles were generated with a range of simulated WT (1–5 mm) and attenuations (–100 HUs to +100 HUs in 10-HU increments). Figure 1 shows examples of three profiles used in our experiment, each with a real wall area (WA) = –50 HUs and real WT of 1.5, 2.5, and 4 mm. The low-pass characteristic of the PSF was observed to introduce a blurring that reduces the intensity contrast of structures whose size is the order of the PSF size. For each simulated airway and its corresponding profile, measured WT was calculated using the full-width at half-maximum (FWHM) method of edge detection (1). Airway wall attenuation was defined as the PWAt in the intensity profile, as depicted by the arrows in Fig. 1.

**Phantom CT and NLST CT analysis.** The four tubes representing simulated airways were visually identified and analyzed in a single axial image of the COPDGene phantom. In the clinical images, airway RB1, the apical segment of the right upper lobe (AS-RUL) was identified for each subject.

For both the phantom and clinical CT scans, a seed point was manually placed in the airway lumen, and its centroid was automatically calculated. From the centroid, 128 one-dimensional (1D) rays were cast in 360°. The sampled 1D profiles through the airway wall were then interpolated using a cubic B-spline (11, 13) with a resolution of 0.05 mm. The lumen-wall and wall-parenchymal boundaries for each 1D profile were determined using the standard FWHM method for edge detection (9, 14). The metrics of the airway wall collected included mean lumen area (LA), WT, WA percent (WA%; defined as  $100 * WA / \text{total cross-sectional area of wall and lumen}$ ), and mean PWAt. Measures of mean peak airway wall attenuation were determined by averaging the peak attenuation values of the mural portion of each 1D profile (Fig. 3). In each subject, a single measure of RB1 airway morphology was collected and is reported as RB1 WT, PWAt, etc.

For the phantom images, tube morphology was calculated as an average of the values obtained from the full 128 rays. Where possible, circumferential measures of the airway wall were collected for the in vivo CT scans. In places in which the outer airway wall boundary was obscured by an adjacent vessel, only those regions of the airway that visually appeared to have undergone acceptable segmentation using the FWHM method were included in the analysis.

Airway analysis was performed by one of the authors (A. Diaz), who was blinded to measures of lung function. Standard densitometric measures of emphysema were performed as described previously using a HU threshold of –950 (6). Quantitative image analysis was performed using Airway Inspector ([www.airwayinspector.org](http://www.airwayinspector.org)).

This study received approval from the Institutional Review Board at Brigham and Women's Hospital.

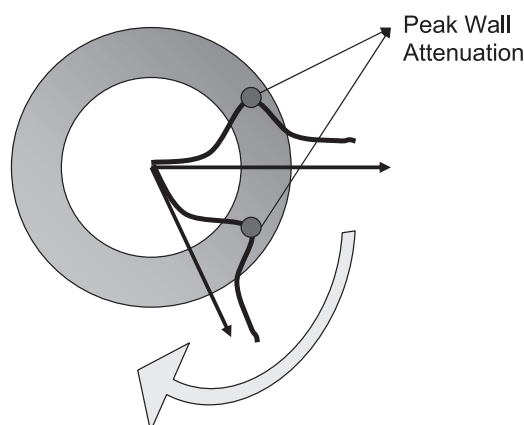


Fig. 3. The mean PWAt was calculated by taking the mean of the peak attenuation along each ray, radiating outward from the centroid of the airway lumen. In the case of circumferential measures of the airway wall, the PWAt would be a mean of the peak attenuation of the mural portion of 128 one-dimensional rays.

### Statistical Analysis

Baseline characteristics of the study cohort are presented as means  $\pm$  SD and were compared using *t*-tests. Spearman correlation coefficients were used to express the relationship between CT measures of airway disease and lung function. Additional multivariate linear regression modeling was performed to assess the relationship of lung function and CT-based measures of emphysema and airway disease. *P* values < 0.05 were considered statistically significant. Data analysis was performed using SAS version 9.1 (SAS Institute, Cary, NC).

## RESULTS

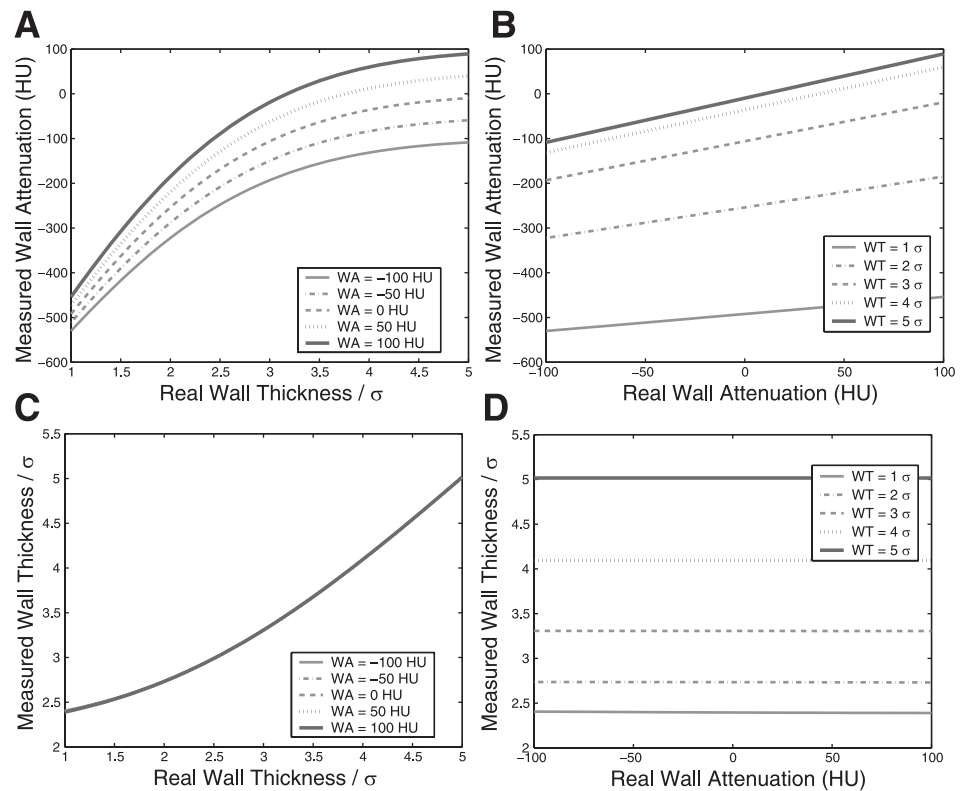
### Computer Simulation

The results of the computer-based simulation study are provided in Fig. 4. Measurements of WT are provided as a function of the sigma (where sigma is the standard deviation of the Gaussian distribution representing the PSF and is equal to 1 mm) of the simulated PSF of the image. As shown in Fig. 4, *A* and *B*, there is universal underestimation of the true mural attenuation when using the CT-derived PWAt measures for all airway walls, and it is not until the actual airway WT approaches 5 sigma of the PSF that the measured and actual PWAt values are in agreement. Furthermore, the data presented in Fig. 4*B* suggest that, for a fixed WT, there is a linear relationship between real and observed PWAt, even in airway walls less than five times sigma. Figure 4*C* depicts the curvilinear relationship between actual and measured WT. Again, it is not until the real airway WT approaches 5 sigma of the PSF that there is agreement between the actual and measured thickness. Finally, Fig. 4*D* depicts the relationship between the actual wall attenuation and measured WT. Note that variations in the actual airway wall attenuation do not influence airway WT measures when using the FWHM method; FWHM appears to be insensitive to changes in structure density.

### Phantom Validation

Four tubes representing a range of simulated airway sizes were analyzed (Fig. 2). The phantom tubes were segmented using the FWHM algorithm for edge detection, and the mea-

Fig. 4. Results of computer-based simulation study. *A*: the relationship between the real wall thickness (WT; normalized by the sigma of the PSF where sigma = 1 mm) and the measured mean PWAt for a series of airways with expected wall attenuations of -100 to +100 HUs. *B*: the linear relationship between the real and measured PWAt for a series of airway walls [ranging from 1 to 5 times the sigma of the point spread function (PSF)]. *C*: the relationship between real WT (normalized for the sigma of the PSF) and that measured using the full-width at half-maximum (FWHM) technique (again, normalized by the sigma of the PSF) on a CT image. *D*: for a given WT, changes in the real airway wall attenuation (PWAt) do not influence measured thickness using the FWHM technique. WA, wall area.



tures obtained were compared against the manufacturer's specifications (Table 1, Figs. 5). As shown, there is marked overestimation in WT in all tubes, although the degree of overestimation is greater in the smaller airways.

Figure 5B depicts the relationship between observed and expected PWAt for each tube, where the expected attenuation of the polycarbonate is 180 HUs. There was uniform underestimation of the expected polycarbonate attenuation when using the PWAt values acquired with the FWHM method, and this effect was greatest in the smallest phantom airway.

#### Cohort Demographics

A total of 224 subjects (93 women, 131 men) with CT scans and corresponding prebronchodilator spirometry were included in this investigation. Demographics, smoking history, and the distribution of GOLD stages are provided in Table 2. Subjects with GOLD 3 and 4 diseases were pooled into one group (GOLD 3&4) due to limited numbers of subjects with GOLD stage 4 disease.

#### NLST Airway Phenotypes

Measures of airway WT tended to be inversely related to the forced expiratory volume in 1 s ( $FEV_1$ ) expressed as percent predicted ( $FEV_1\%$  predicted) ( $r = -0.13$ ,  $P = 0.06$ ), although the trend did not meet statistical significance. The WA%, LA, and the PWAt were statistically significantly inversely correlated with the  $FEV_1\%$  predicted (WA%:  $r = -0.28$ ,  $P < 0.0001$ ; LA:  $r = 0.14$ ,  $P = 0.03$ ; and PWAt:  $r = -0.18$ ,  $P = 0.0008$ , respectively). The forced vital capacity (FVC) expressed as percent predicted ( $FVC\%$  predicted) was significantly correlated with three CT measures of airway disease (WT:  $r = -0.19$ ,  $P = 0.05$ ; WA%:  $r = -0.33$ ,  $P < 0.0001$ ; PWAt:  $r = -0.27$ ,  $P < 0.0001$ ), but not LA ( $r = 0.04$ ,  $P = 0.52$ ). Last, none of the CT metrics of airway disease WT, WA%, LA, or PWAt were predictive of the ratio of the subject's  $FEV_1$  and FVC ( $FEV_1/FVC$ ) (WT:  $r = -0.05$ ,  $P = 0.41$ ; WA%:  $r = -0.014$ ,  $P = 0.83$ ; LA:  $r = 0.07$ ,  $P = 0.30$ ; PWAt:  $r = -0.11$ ,  $P = 0.11$ ). In additional multivariate

Table 1. Manufacturer specifications and measured values for the computed tomography phantom, including lumen radius, wall thickness, and wall attenuation

Tube No.	Lumen Radius (Manufacturer), mm	Wall Thickness (Manufacturer), mm	Wall Thickness FWHM (SD), mm	Wall Attenuation (Manufacturer), HU	Measured mpWA (SD), HU
1	1.5	0.6	1.4 (0.07)	180	-554 (86)
2	3	0.9	1.4 (0.06)	180	-368 (121)
3	3	1.2	1.57 (0.04)	180	-276 (136)
4	3	1.5	1.74 (0.06)	180	-210 (148)

SD values are in parentheses. The tubes were all constructed from the same material and are thus of the same "true" attenuation. FWHM, full-width at half-maximum; mpWA, mean peak wall attenuation; HU, Hounsfield units.

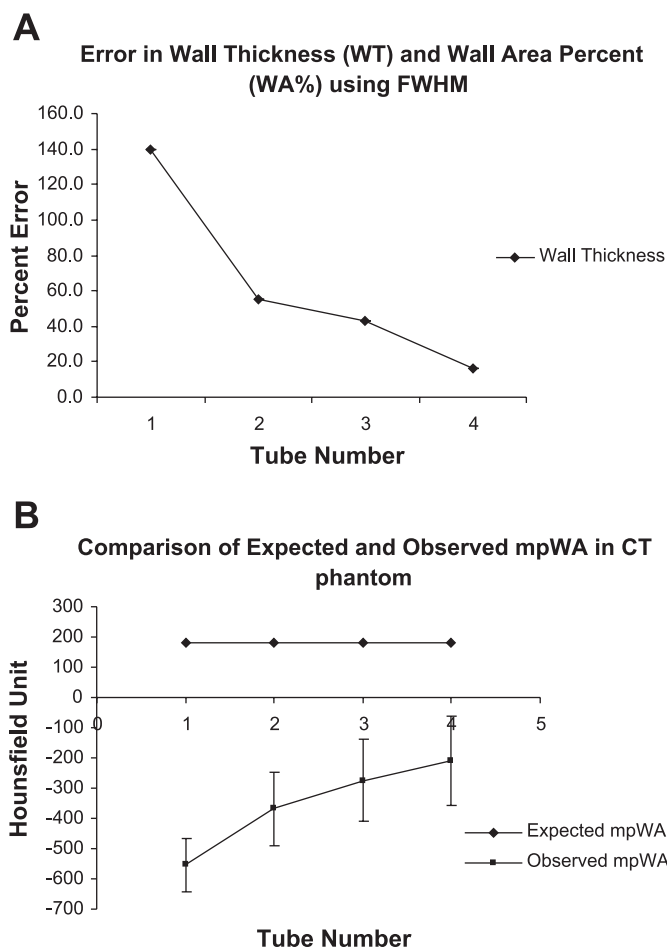


Fig. 5. A: the error in WT estimation using the FWHM method for edge detection. The greatest error (~140%) was observed in the smallest airway. B: comparison of expected WT and associated CT attenuation values with those obtained experimentally. Note that error bars represent the SD of the circumferential measures of PWAt. mpWA, mean peak wall area.

modeling using CT measures of emphysema and airway disease to predict lung function, measures of PWAt remained as a statistically significant predictor of the FEV<sub>1</sub>% predicted when adjusted for both WA% and percent emphysema (Table 3). The model coefficient of determination was 0.31.

## DISCUSSION

Previously, Dougherty and Newman (5) proposed using CT-derived measures of PWAt of cortical bone as a metric of its structural properties. Based on their work, we sought to examine the utility of airway wall PWAt as a CT-based measure of airway disease in subjects with COPD. Using a computer-based simulation study and CT phantom, quantitative assessments of mean PWAt were performed, and their relationship to WT and expected wall attenuation was examined. After evaluating the performance of this metric in these preliminary investigations, measures of PWAt, WT, and WA% were performed in the AS-RUL of a cohort of subjects participating in the NLST and correlated to spirometric measures of lung function. On univariate analysis, measures of PWAt appeared to be a stronger correlate to lung function than WT and of comparable strength to WA% in its relationship to the

Table 2. Demographic information and measures of lung function for the pooled study cohort and by sex

Characteristic	
Male sex, no.	131 (58%)
Age, yr	62 ± 5
FEV <sub>1</sub> , %predicted	76 ± 20
FVC, %predicted	92 ± 16
FEV <sub>1</sub> /FVC	0.65 ± 0.13
Active smoker, no.	123 (55%)
Pack·yr tobacco	51 (35–60)
Normal spirometry, no.	81
GOLD 1, no.	39
GOLD 2, no.	74
GOLD 3&4, no.	30
LAA –950 HUs, %	6.4 (6.4)
Lumen area, mm <sup>2</sup>	8.6 (3.4)
Wall thickness, mm	2.4 (0.4)

Values represents the cohort of 224 subjects, unless specified, and are means ± SD, with the exception of pack·yr smoking history, which is provided as medians and interquartile ranges. FEV<sub>1</sub>, forced expiratory volume in 1 s; FVC, forced vital capacity; GOLD, Global Initiative for Chronic Obstructive Lung Disease, LAA, low-attenuation area.

FEV<sub>1</sub>% predicted, FVC% predicted, and the FEV<sub>1</sub>/FVC. With additional multivariate modeling, PWAt remained as a significant predictor of lung function after being adjusted for WA% and percent emphysema. The results of this univariate and multivariate analysis suggest that PWAt may capture additional phenotypic information regarding CT measures of airway disease not assessed by either WT or WA%.

In chronic inflammatory conditions such as COPD, airway disease can manifest as mural remodeling with proximal airway wall thickening, and it is such thickening that is utilized as an image-based measure of disease (15, 23). The authors postulate that this chronic remodeling process may also result in an increase in tissue density or CT attenuation. Behar and colleagues (3) reported that subjects with the chronic inflammatory condition relapsing polychondritis affecting the lower respiratory tract were observed to have airway walls of increased X-ray attenuation on CT scan. The etiology of this observation was not validated histologically, but was thought to be due to mural calcification and fibrosis (3). More recently, using optical coherence tomography, Coxson and colleagues (4) made the subtle observation that a subject with greater expiratory airflow obstruction had increased mural density in the subepithelial region, which they believed to be due to increased collagen deposition characteristic of chronic airway remodeling (4). While such a finding is likely beyond the resolution of clinical CT scanning, it does support a hypothesis that mural remodeling may influence airway wall density.

Table 3. Results of multivariate modeling using WA%, peak wall attenuation, and densitometric measures of emphysema to predict a subject's FEV<sub>1</sub>% predicted

	β Coefficient	P Value
WA%	–0.89	<0.0001
mpWA	–0.03	0.018
%Emphysema (950-HU threshold)	–144.84	<0.0001

The model coefficient of determination ( $R^2$ ) was 0.31. WA%, wall area percent.

When considered in the context of a standardized CT protocol, mean PWAt is a function of two unique structure properties: size and density. When evaluated individually, PWAt underestimated true attenuation in a nonlinear fashion, with the greatest error observed in the smallest airways. Such observations are consistent with the concept of contrast reduction (22) and validate the performance of our computer simulation. The simulation results further suggest that, for a given structure size, measured PWAt is linearly related to true PWAt and, while inaccurate, exhibit no differential bias across the range of simulated "real" attenuations (Fig. 4B). The ability of PWAt to simultaneously assess both thickness and density, therefore, appeared to be robust and supported its application in further clinical investigation. It is possible that the correlative strength of PWAt observed in our multivariate modeling was due to its ability to assess not only WT through the partial volume effect, but also subtle changes in wall attenuation associated with the process of airway remodeling. The latter conjecture on the part of the authors is, however, less likely, given the contrast resolution of clinical CT imaging. Further histopathological investigation is needed to support such a theory.

There are technical limitations of this investigation that must be noted. The CT data were not optimal for quantitative assessments of airway wall structure. Both the partial volume averaging inherent in increasing slice thickness and the lower spatial frequency of the "smoother" standard reconstruction algorithm significantly bias our airway measurements to overestimate true WT. In an attempt to minimize this bias, airway measures were only taken from the AS-RUL, because its long axis generally runs perpendicular to axial image acquisition. While measurements confined to this site will not address issues related to the reconstruction algorithm, it will, in part, mitigate the partial volume effect inherent to airway analysis in thicker CT images.

A further limitation of this investigation is the narrow range of sizes of airways assessed in the NLST cohort (WT > 2 mm) and their inability to adequately assess the relative merits of PWAt against either WT or WA%. As shown in Fig. 4C, any discrete range of real airway sizes may fall into a roughly linear portion of the curve, depicting the relationship of observed and expected WT. Because of this, the mural thickening in the AS-RUL is likely detected as a proportional change in CT assessments of the same. In such cases, one would not expect PWAt to be clearly superior to measures of WT in correlative analysis. A broader range of airways whose size spans a nonlinear part of the curve in Fig. 4C, specifically the flatter region of the curve at smaller WT, where CT may lack the ability to accurately discriminate changes in WT, must be examined to assess the true merits of PWAt.

A limitation of PWAt as a measure of airway disease used in correlative investigation must also be discussed. While CT measures of disease are focused on proximal airway wall thickening, it is consistently observed that airway WT is a poor indicator of lung function (9, 14). WT does not specifically predict LA, the latter being the main component to resistance to airflow in the lung. To address this, the standard CT measure of disease has become WA%, a metric based on both WA and its corresponding LA. The current measurement of PWAt does not specifically take into account a reduction in LA, and, as such, a more valid comparison can be made between WT and

PWAt than between WA% and PWAt. Further work is needed to derive a "lumen adjustment" for PWAt to adequately assess its performance against WA% in correlative analysis.

COPD is recognized as being a heterogeneous syndrome of airway disease and emphysema, leading to incompletely reversible expiratory airflow obstruction (16). In addition to the unpredictable admixture of these disease processes in any one individual, there is a tremendous variability in subject symptoms and response to therapeutic intervention (7, 10). Because of this, there are increasing efforts to define more homogeneous subsets of subjects and potentially define new biomarkers that facilitate clinical investigation. Inherent to that effort is the identification of CT-based metrics of airway disease that can increasingly predict subject disease state. Thus the detection and validation of a metric that augments current efforts in imaged-based quantification of disease would be of great use. Mean peak airway wall attenuation appears to offer an easily quantifiable and reproducible metric of airway disease in subjects with COPD. The advantage of this measure of disease over current standards includes its ability to detect changes in both WT and density that may be associated with airway disease. Further investigation is required to determine its histopathological correlate and utility in the smaller airways at the limits of current clinical CT scanner resolution.

#### GRANTS

G. R. Washko was supported by National Heart, Lung, and Blood Institute (NHLBI) Grants 1K23HL089353-01A1, 5U10HL074428-05, U01 HL089897, and U01 HL089856, and a grant from the Parker B. Francis Foundation. Funding for the CT phantom was provided by Siemens and NHLBI Grants U01-HL089897 and U01-HL089856.

#### REFERENCES

1. Amirav I, Kramer SS, Grunstein MM, Hoffman EA. Assessment of methacholine-induced airway constriction by ultrafast high-resolution computed tomography. *J Appl Physiol* 75: 2239–2250, 1993.
2. [Anon]. Standardization of Spirometry, 1994 Update. American Thoracic Society. *Am J Respir Crit Care Med* 152: 1107–1136, 1995.
3. Behar JV, Choi YW, Hartman TA, Allen NB, McAdams HP. Relapsing polychondritis affecting the lower respiratory tract. *AJR Am J Roentgenol* 178: 173–177, 2002.
4. Coxson HO, Quiney B, Sin DD, Xing L, McWilliams AM, Mayo JR, Lam S. Airway wall thickness assessed using computed tomography and optical coherence tomography. *Am J Respir Crit Care Med* 177: 1201–1206, 2008.
5. Dougherty G, Newman D. Measurement of thickness and density of thin structures by computed tomography: a simulation study. *Med Phys* 26: 1341–1348, 1999.
6. Dransfield MT, Washko GR, Foreman MG, Estepar RS, Reilly J, Bailey WC. Gender differences in the severity of CT emphysema in COPD. *Chest* 132: 464–470, 2007.
7. Fishman A, Martinez F, Naunheim K, Piantadosi S, Wise R, Ries A, Weinmann G, Wood DE. A randomized trial comparing lung-volume-reduction surgery with medical therapy for severe emphysema. *N Engl J Med* 348: 2059–2073, 2003.
9. Hasegawa M, Nasuhara Y, Onodera Y, Makita H, Nagai K, Fuke S, Ito Y, Betsuyaku T, Nishimura M. Airflow limitation and airway dimensions in chronic obstructive pulmonary disease. *Am J Respir Crit Care Med* 173: 1309–1315, 2006.
10. Jones PW. Health status measurement in chronic obstructive pulmonary disease. *Thorax* 56: 880–887, 2001.
11. Lehmann TM, Gonner C, Spitzer K. Survey: interpolation methods in medical image processing. *IEEE Trans Med Imaging* 18: 1049–1075, 1999.
12. Miller MR, Hankinson J, Brusasco V, Burgos F, Casaburi R, Coates A, Crapo R, Enright P, van der Grinten CP, Gustafsson P, Jensen R, Johnson DC, MacIntyre N, McKay R, Navajas D, Pedersen OF,

- Pellegrino R, Viegi G, Wanger J. Standardisation of spirometry. *Eur Respir J* 26: 319–338, 2005.
13. Mitchell DPNA. *Reconstruction Filters in Computer-Graphics*. New York: ACM, 1988.
14. Nakano Y, Muro S, Sakai H, Hirai T, Chin K, Tsukino M, Nishimura K, Itoh H, Pare PD, Hogg JC, Mishima M. Computed tomographic measurements of airway dimensions and emphysema in smokers. Correlation with lung function. *Am J Respir Crit Care Med* 162: 1102–1108, 2000.
15. Nakano Y, Wong JC, de Jong PA, Buzatu L, Nagao T, Coxson HO, Elliott WM, Hogg JC, Pare PD. The prediction of small airway dimensions using computed tomography. *Am J Respir Crit Care Med* 171: 142–146, 2005.
16. Patel BD, Coxson HO, Pillai SG, Agusti AG, Calverley PM, Donner CF, Make BJ, Muller NL, Rennard SI, Vestbo J, Wouters EF, Hiorns MP, Nakano Y, Camp PG, Nasute Fauerbach PV, Screaton NJ, Campbell EJ, Anderson WH, Silverman EK, Lomas DA. Airway wall thickening and emphysema show independent familial aggregation in chronic obstructive pulmonary disease. *Am J Respir Crit Care Med* 178: 500–505, 2008.
17. Rabe KF, Hurd S, Anzueto A, Barnes PJ, Buist SA, Calverley P, Fukuchi Y, Jenkins C, Rodriguez-Roisin R, van Weel C, Zielinski J. Global strategy for the diagnosis, management, and prevention of chronic obstructive pulmonary disease: GOLD executive summary. *Am J Respir Crit Care Med* 176: 532–555, 2007.
18. Reinhardt JM, D'Souza ND, Hoffman EA. Accurate measurement of intrathoracic airways. *IEEE Trans Med Imaging* 16: 820–827, 1997.
20. San Jose Estepar R, Washko G, Silverman E, Reilly J, Kikinis R, and Westin C-F. Accurate airway wall estimation using phase congruency. In: *R Larsen, M Nielsen, and J Sporning Lecture Notes in Computer Science; Oct 2006 Meeting*. Berlin: Springer, 2006, p. 125–134.
21. Schwarzband G, Kiryati N. The point spread function of spiral CT. *Phys Med Biol* 50: 5307–5322, 2005.
22. Shuping RE, Judy PF. Resolution and contrast reduction. *Med Phys* 5: 491–496, 1978.
23. Tiddens HA, Pare PD, Hogg JC, Hop WC, Lambert R, de Jongste JC. Cartilaginous airway dimensions and airflow obstruction in human lungs. *Am J Respir Crit Care Med* 152: 260–266, 1995.
24. Wang G, Skinner MW, Vannier MW. Temporal bone volumetric image deblurring in spiral computed tomography scanning. *Acad Radiol* 2: 888–895, 1995.
25. Washko GR, Dransfield MT, San Jose Estepar R, Diaz A, Silverman EK, Bailey WC, Reilly JJ. Airway wall intensity: a novel CT based metric of airway disease in COPD (Abstract). *Am J Respir Crit Care Med* 177: A285, 2008.
26. Zerhouni EA, Spivey JF, Morgan RH, Leo FP, Stitik FP, Siegelman SS. Factors influencing quantitative CT measurements of solitary pulmonary nodules. *J Comput Assist Tomogr* 6: 1075–1087, 1982.

